Nuclear Instruments and Methods in Physics Research B 317 (2013) 121–125

Contents lists available at SciVerse ScienceDirect

Nuclear Instruments and Methods in Physics Research B

journal homepage: www.elsevier.com/locate/nimb

Experimental resolution of deuterium and hydrogen depth profiling with the nuclear reactions D(^{3}He,p)α and p(^{15}N,α,γ)^{12}C

S. Bielesch [a], M. Oberkofler [a,*], H.-W. Becker [b], H. Maier [a], D. Rogalla [b], T. Schwarz-Selinger [a], Ch. Linsmeier [a]

[a] Max-Planck-Institut für Plasmaphysik, EURATOM Association, Boltzmannstr. 2, 85748 Garching, Germany
[b] Dynamitron Tandem Labor des RUBION, Ruhr-Universität Bochum, 44780 Bochum, Germany

ARTICLE INFO

Article history:
Received 18 October 2012
Received in revised form 1 February 2013
Accepted 1 February 2013
Available online 11 February 2013

Keywords:
Depth resolution
NRA analysis

ABSTRACT

In this paper well defined test samples are used to show how the analysis depth and the matrix material influence the depth resolution of nuclear reaction analysis. The reaction D(^{3}He,p)α is used to detect deuterium. By covering 10 nm thin deuterated amorphous carbon (a–C:D) films on silicon with tungsten (Z_W = 74) and titanium (Z_{Ti} = 22) of various thicknesses between 500 nm and 8 μm the influence of the atomic number and the overlayer thickness on the depth resolution is studied. The most probable depth profiles are calculated from the experimental data with the program NRADC, which implements Bayesian statistics. The resulting apparent layer width of the deuterium containing layer broadens with increasing thickness of the coating and this broadening is more pronounced for coatings with higher Z. These apparent layer widths are a measure for the experimentally achievable depth resolution. Their absolute values are in the same range as the theoretical optimum calculated with RESOLNRA. To investigate the depth resolution of the p(^{15}N, α, γ)^{12}C reaction, a 12 nm thin hydrogenated amorphous carbon (a–C:H) film on silicon and a pure tungsten sample are analysed. The width of the instrument function of this method is deduced from the surface hydrogen peak of the pure tungsten sample. The two methods are compared.

1. Introduction

In a previous work we have investigated the depth resolution of different ion beam analysis methods for detecting near-surface deuterium [1]. In greater depths the resolution deteriorates due to geometrical and electronic straggling. In this work we experimentally determine the depth-dependence of the resolutions achievable with common nuclear reaction analysis (NRA) methods for hydrogen isotope detection.

The two most common reactions for detecting the hydrogen isotopes deuterium and protium are shown in Eqs. (1) and (2).

$$D(^3He, p)\alpha \quad (1)$$

$$p(^{15}N, \alpha, \gamma)^{12}C \quad (2)$$

Both reactions provide high sensitivity with cross section maxima of 60 mb/sr (at a scattering angle of 135°) and 1650 mb (integral cross section) respectively and feature a peaked cross section. The latter allows a variation of the depth which is dominantly probed in a NRA measurement: The depth at which the particles from the analysing ion beam reach the energy of the maximum in the NRA cross section can be varied by changing the energy of the analysing beam. In the case of D detection this technique is commonly applied to measure deuterium depth profiles up to depths of several μm [2,3]. However, the resonance of reaction (1) has a width of about 500 keV and the peak of the cross section, at the resonance energy of 630 keV, is merely a factor of 6 above the off-resonance contributions at higher energies [2,4]. The resulting considerable non-resonant contributions in the spectra make a correct interpretation of such measurements challenging. A proper analysis of the measured spectra requires deconvolution of the experimental data. This deconvolution is done here with the recently developed program NRADC [5].

Compared to reaction (1), reaction (2) has a very narrow resonance at 6385 keV with a width of 1.8 keV. The off-resonance cross section drops by four orders of magnitude [6]. Therefore, in this case to a good approximation every beam energy probes only a very narrow depth interval and no deconvolution of the spectra acquired at various energies is necessary.

As well-defined model systems for these investigations approximately 10 nm thin deuterated armorphous carbon films (a–C:D) on silicon substrates are used. These films are buried under W or Ti layers of various thicknesses. The D or H concentration profiles can be described by delta functions if the thickness of the D- or H-containing layer is well below the depth resolution of the analysis method. The resulting experimental depth profiles then represent response functions of the applied method and the broadening of the delta profile is a measure of the depth resolution.

* Corresponding author. Tel. +49 89 3299 1005.
E-mail address: martin.oberkofler@ipp.mpg.de (M. Oberkofler).

0168-583X/$ - see front matter © 2013 Elsevier B.V. All rights reserved.
http://dx.doi.org/10.1016/j.nimb.2013.02.003

2. Experimental

2.1. Sample preparation

Amorphous hydrogenated (deuterated) thin carbon films (a–C:H and a–C:D, respectively) were grown on Si (0 0 1) substrates on the driven electrode of an asymmetrical capacitively coupled discharge (13.56 MHz) using methane with a purity of 99.995% or deuterated methane with an enrichment of 99.94%. A discharge pressure of 2.0 Pa and a DC self bias of −300 V was applied.

Growth was monitored in situ by reflectometry at 632 nm wavelength. For these growth conditions, so-called dense a–C:H (a–C:D) films are expected to grow. This was confirmed by measurements of the refractive index and the absorption of the films ex situ by ellipsometry at 632 nm wavelength yielding a complex refractive index of $\hat{n} = 2.15 - i \times 0.1$ for the a–C:H and $\hat{n} = 2.03 - i \times 0.05$ for the a–C:D films. For a–C:H films the strong correlation of the refractive index in the visible range with the carbon density ρ_C and the hydrogen content $H/(H+C)$ allows to deduce these values [7] yielding $H/(H+C) = 33\%$ and a $\rho_C = 9.2 \times 10^{28}$ m^{-3}.

A recent ion beam analysis study reveals similar $H/(H+C)$ and $D/(D+C)$ ratios of films deposited from CH_4 and CD_4 with the same parameters but carbon and hydrogen density in the films turn out to be lower for the deuterated films [8]. This observation was confirmed here independently by growing 300 nm thick a–C:H and a–C:D films under identical growth conditions (−300 V self-bias, 2.0 Pa neutral pressure, identical pumping speed) and measuring the mass increase due to the deposition ex-situ by a microbalance. The film thickness was determined locally with interferometry in situ as well as laterally resolved with tactile profilometry ex situ. While the a–C:H film had a density of 1.8 g/cm^3 the a–C:D film showed 1.7 g/cm^3.

For this study 10 nm thick a–C:D films were used for the ^{3}He measurements and 12 and 330 nm thick a–C:H films were used for the ^{15}N experiments.

The a–C:D films used to investigate the influence of overlayers on the depth resolution are covered with tungsten and titanium of various thicknesses between 500 nm and 8 μm. These films are prepared by DC magnetron sputter deposition. Argon is used as a working gas for the sputtering process. The deposition occurs at an argon gas pressure of 0.8 Pa and a voltage of −340 V at the sputter target. These parameters are chosen to create as smooth as possible deposits and to avoid stress in the films. Before the deposition of the metallic deposits the a–C:D surface is sputter cleaned applying a RF self bias of −570 V and a pressure of 0.5 Pa for 60 s. Due to this cleaning, the thickness of the a–C:D films is reduced by a few nm and hence cannot be quantified exactly. The thicknesses of the titanium or tungsten coatings are measured by tactile profilometry on suitable reference samples which were exposed simultaneously in each deposition run. Using the thicknesses measured by profilometry and areal densities from Rutherford backscattering (RBS) analysis, it is possible to calculate the atomic densities of the sputtered deposits with Eq. (3).

$$\text{atomic density} = \frac{\text{thickness measured with RBS [at/cm}^2\text{]}}{\text{thickness measured with profilometry [cm]}} \quad (3)$$

The resulting atomic densities are 5.8×10^{22} cm^{-3} for tungsten and 4.4×10^{22} cm^{-3} for titanium. For comparison, the respective values for the pure bulk elements are 6.3×10^{22} cm^{-3} for tungsten and 5.7×10^{22} cm^{-3} for titanium [9].

2.2. Nuclear reaction analysis

2.2.1. ^{3}He reaction

The NRA measurements using reaction (1) are performed at the 3 MV tandem accelerator at IPP Garching. To determine the D concentration at different depths proton spectra from the D(^{3}He,p)α nuclear reaction are measured for different ^{3}He energies between 500 and 6000 keV. A wide-angle high-energy-resolution proton detector is mounted at a scattering angle of 135°. In order to improve depth resolution an aperture with a curved slit is placed in front of the detector resulting in a solid angle of 29.94 msr. A Ni absorber foil with a thickness of 5 μm and 12 μm Mylar foil are additionally positioned in front of the detector to absorb elastically scattered ^{3}He ions and α particles from the D(^{3}He,p)α nuclear reaction. For each NRA spectrum a total charge of 10 μC is acquired on a spot size of 1 mm^2 applying a beam current of 20 nA. The energy calibration is done with the proton signal from the D(^{3}He, p)α reaction and the three proton peaks from the ^{12}C(^{3}He, p)^{14}N reaction, which appear at primary ^{3}He energies above 2400 keV.

2.2.2. ^{15}N reaction

The NRA measurements using reaction (2) are performed at the 4 MV tandem accelerator at the RUBION facility in Bochum. The gamma rays of the reaction are detected with a 30 × 30 cm^2 NaI(Ti) detector. More information about the experimental setup is given in [10]. As a first experiment a 330 nm thick a–C:H film is analysed to ensure that the selected ion beam parameters used yield a sufficient counting statistics without depleting the sample of hydrogen. Thirteen measurements with a charge of 0.02 μC each are performed at a single position on the sample with a beam energy of 6700 keV, a current of 800 pA and a beam footprint of 7 mm^2. Since the resulting count rates from all these measurements coincide within the error bars, a current of 800 pA is used throughout the analysis. The collected charge per measurement point is 0.04 μC for the a–C:H samples and 2.6 μC for the tungsten sample.

For the determination of the H depth profiles in the a–C:H samples energy scans are performed. The beam energy is raised from 6395 keV up to a value of 6500 keV. The stepwise increase of the analysing energy is tailored to the depth region of interest. Smaller steps in energy are chosen around energies probing a depth where strong gradients in the hydrogen concentration are expected. The same procedure was used for the determination of the H surface peak stemming from adsorbed H_2O on a pure tungsten sample. Background spectra are recorded during the measurement outside the region where the gamma rays stemming from the hydrogen are expected and then subtracted from the counts in the region of interest to account for other gamma rays in the spectra, e.g. from cosmic radiation.

3. D depth profiling with ^{3}He NRA

3.1. Finding the optimal analysis energies

NRA spectra at various analysing energies are recorded from each sample during the experimental determination of the D depth distribution. Due to limited experimental time, it is advisable to optimize these analysing energies with the criterion to get most information about the investigated sample out of a given number of measurements at a given analysis fluence. As a reasonable trade-off between achievable accuracy of the depth profiles and expenditure of time, five measurements at a fluence of 10 μC are performed. Due to the various top-layer thicknesses the most useful energies vary between the different samples. The choice of the most useful energies for each sample is objectified by applying a numerical code based on Bayesian statistics which has been

designed explicitly for the optimization of NRA depth profiling [4]. In this special case the D depth profiles are known beforehand and all 5 energies to be used can be calculated without any input of experimental NRA data. As input for the optimization calculations the following parameters are specified:

- the known D depth profile,
- the material of the cover layer.
- the element constituting the analysis beam,
- the first analysing energy, and
- the geometry of the experiment.

The (known) depth profile is modelled as a product of step functions. The properties of the analysed material are the atomic number, mass and density. As starting energies 6000 keV for tungsten and 4200 keV for titanium are chosen, since these energies are high enough to penetrate through the thickest produced cover layers. With this information the program calculates the next energy, at which to measure, in order to get a maximum of information. This calculated energy is then used as the second measurement energy by the program. In this way the five most useful measurement energies are calculated for each sample. For the samples with tungsten coatings of 6 or 8 μm, the fifth calculated measurement energy is the same as the fourth. Apparently, in these cases it is more beneficial to improve the statistics at the given energy, than to measure at an additional energy. The resulting measurement energies used are given in Table 1.

3.2. Finding the 'most probable' depth profile

Each set of experimental spectra acquired on one sample is deconvoluted into a depth profile with the help of the program NRADC [5]. This program calculates the most probable depth profile from a given number of experimental data by using Bayesian statistics. To this aim the forward calculation of NRA spectra from a given depth profile is linearized by setting up a design matrix. The elements of this matrix are calculated with SIMNRA [11]. As target for the calculation pure tungsten or pure titanium is used, since the thickness of the a–C:D layer is negligible compared to the cover thicknesses. Another necessary input is an initial depth sampling. The same sampling is chosen for all samples: The total layer thickness is divided into 740 sublayers with a thickness of 100×10^{15} cm^{-2}. Using the calculated atomic densities of Section 2.1 the thicknesses correspond to 17 nm in W and 22 nm in Ti. Based on Occams Razor's principle NRADC merges these sublayers into the most probable depth profile given the experimental data.

As an example, Fig. 1 shows the proton integrals and proton spectra at all analysis energies for the a–C:D film covered with 500 nm tungsten. The open squares represent the measured data. The filled circles respectively lines result from a forward calculation performed within NRADC on the basis of the resulting most probable depth profile. The NRADC results are in good agreement with the measured data (the reduced $\chi^2 = 1.2$). In Fig. 2 the corresponding depth profile is plotted (dashed line). This result is compared to the depth profile (solid line), which is known from profilometry and interferometry. The total amounts of deuterium (integrals over the two depth profiles) differ by 7%, which is within the accuracy of the measurement. This provides a consistency check for the NRADC calculations. The D-rich layer of the resulting depth profile has a thickness of 400 nm at a depth from roughly 300 to 700 nm. The depth at which the D-rich layer is located is in good agreement with the known W layer thickness. However, the thickness of the D-rich layer is significantly larger than the actual thickness of approximatly 10 nm. This broadening in the apparent layer width of the deuterium containing layer can be attributed to the depth resolution at this analysis depth in W. According to this result it is not possible to resolve layer thicknesses below 400 nm in a depth of 500 nm using the present technique and geometry.

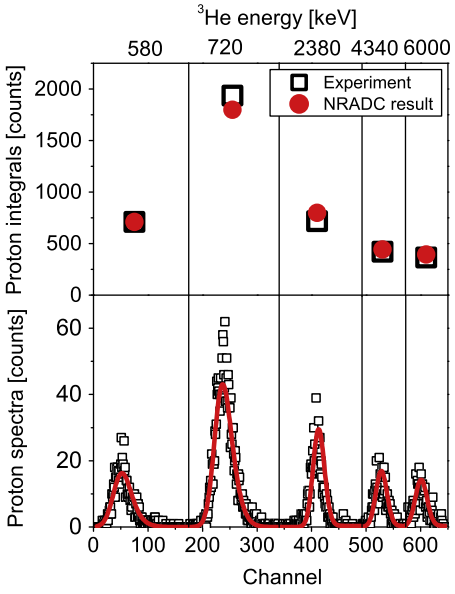

Fig. 1. Comparison of the measured (squares) and calculated (data points or lines) proton spectra (below) and integrals (above) of a 10 nm a–C:D film with 500 nm W coating. In the graph as well as within NRADC the spectra recorded at various energies are strung together along the 'channel'-axis for ease of handling

Fig. 3 shows the results of all measured tungsten samples. The circles indicate the apparent layer widths of the respective layer containing more than 80% of the total deuterium amount, as a function of the thickness of the coating. The remaining 20% (often much less) resides in the long tails, on both sides of the deuterium-rich layer, in concentrations which are several orders of magnitude smaller. On the ordinate the thicknesses are given in 10^{15} cm^{-2}

Table 1
Optimised measurement energies for the different samples.

Coating	E_1 [keV]	E_2 [keV]	E_3 [keV]	E_4 [keV]	E_5 [keV]
No coating	6000	4340	2200	1000	520
W coating					
500 nm	6000	4340	2380	700	580
2000 nm	6000	4600	2700	1640	1560
6100 nm	6000	5060	4040	3540	3540
8000 nm	6000	5060	4460	4340	4340
Ti coating					
500 nm	4200	3180	1720	1200	620
2000 nm	4200	3420	2100	1280	1200
6200 nm	4200	3640	3000	2620	2580

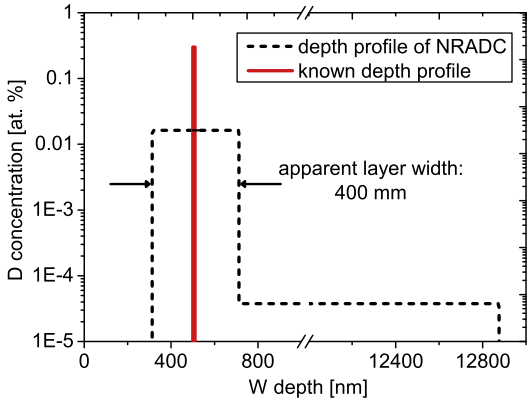

Fig. 2. Comparison of the depth profile known from interferometry and profilometry to the depth profile calculated with NRADC for the 10 nm a–C:D film with 500 nm W coating.

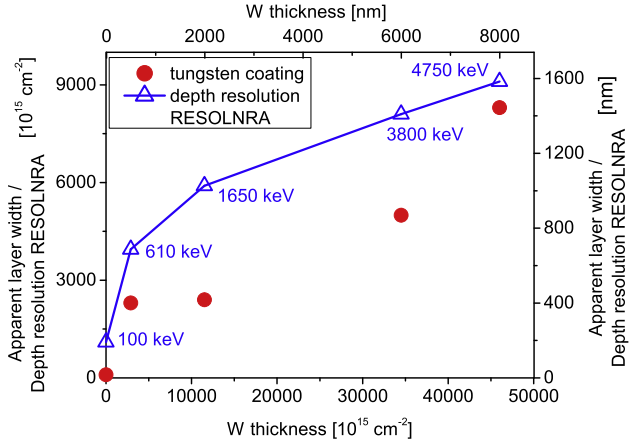

Fig. 3. Apparent layer width (from experiment) and depth resolution (from RESOLNRA calculations) as a function of the thickness of the W coating. The circles show the experimental results. The open triangles are the results from the RESOLNRA calculations at the indicated optimal energies.

(left side) and in nm (right side). The abscissae show the thickness of the coating, again in 10^{15} cm^{-2} (bottom axis) and in nm (top axis). The a–C:D film without any coating can only marginally be resolved in this approach: The apparent layer width of 17 nm is close to the real thickness of approximately 10 nm, but it is at the same time the lower limit given by the initial depth sampling. With increasing thickness of the coating the calculated apparent layer width of the deuterium containing layer increases, reflecting the deterioration of the depth resolution. In Fig. 4 the same is shown for the samples with titanium coating. A comparison of Fig. 3 and Fig. 4 shows that the depth resolution is in most cases inferior for the samples with tungsten coatings. This deterioration for both cover materials can be explained by electronic straggling. For thick cover layers, the electronic straggling dominates, since the geometrical straggling is to a good approximation independent of the depth and therefore constant for the analysed samples. The electronic straggling in the analyzed sample can be described with the Bohr formula (4) [11], which depends on the path length (Δx in units of 10^{18} cm^{-2}) and the atomic numbers of the incoming (Z_1) and the target element (Z_2).

$$\sigma_{\text{Bohr}}\ [\text{keV}] = \sqrt{0.26 \cdot Z_1^2 \cdot Z_2 \cdot \Delta x} \tag{4}$$

The influence of the atomic numbers, in particular of Z_2, is the reason why the depth resolution deteriorates stronger in tungsten ($Z_W = 74$) than in titanium ($Z_{Ti} = 22$). It should be pointed out that the trend of the data shown in Fig. 3 and 4 is not expected to simply follow the Bohr formula. The final depth resolution is influenced by straggling contributions in the analyzed sample for incoming and outgoing particles, as well as straggling in the foil in front of the detector. Ultimately, the experimentally achievable resolution depends on the count statistics for each channel, which is reduced when the proton signal is broadened due to straggling.

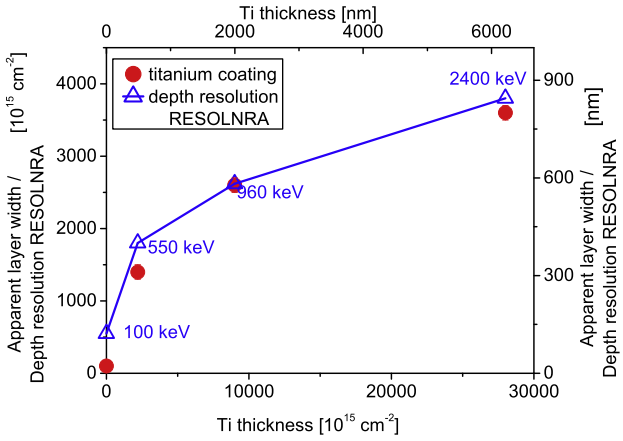

Fig. 4. Apparent layer width (from experiment) and depth resolution (from RESOLNRA calculations) as a function of the thickness of the Ti coating. The circles the experimental results. The open triangles are the results from the RESOLNRA calculations at the indicated optimal energies.

The experimentally obtained apparent layer widths are compared to depth resolution calculations with RESOLNRA [12] in Figs. 3 and 4. The open triangles denote the theoretically achievable resolutions for a single measurement at the indicated optimal analysis energy. The calculated resolutions follow the trend of the experimental layer widths. In the case of titanium even the absolute values coincide, while there is some deviation in the case of tungsten. Part of the scatter in the experimental data is due to the discreteness of the NRADC depth profiles and the somewhat arbitrary fraction of 80% taken for the definition of the D-rich layer. The overall rather good quantitative concordance with the calculated resolutions is very suggestive. However, the experimentally determined layer widths do not directly correspond to depth resolutions as calculated by RESOLNRA: The latter are defined as the full-width-of-half-maximum in the energy spread, converted to a depth interval. The layer widths from the NRADC-deconvolution are, on the other hand, influenced by the measurement statistics as well as straggling mechanisms not properly taken into account by NRADC, such as plural scattering.

4. Comparison to H depth profiling with ^{15}N NRA

To investigate the depth resolution of reaction (2) 12 and 330 nm a–C:H films on silicon and a pure tungsten sample are analysed. With this NRA method no deconvolution is necessary due to the very narrow resonance width (see Section 1). The energy scans are converted into depth profiles with formula (5). In this formula x is the depth, E_{mes} the measurement energy, E_{res} the resonance energy and $\frac{dE}{dx}$ the stopping power.

$$x = \frac{E_{\text{mes}} - E_{\text{res}}}{\frac{dE}{dx}} \tag{5}$$

To determine the unknown stopping power of the a–C:H films, the energy scan of the thick a–C:H film was used. This scan shows a constant elevated hydrogen concentration within the depth of the resonance from 6420 up to 6950 keV. At 7025 keV it has dropped by a factor of 10. The FWHM 'thickness' of the a–C:H film is

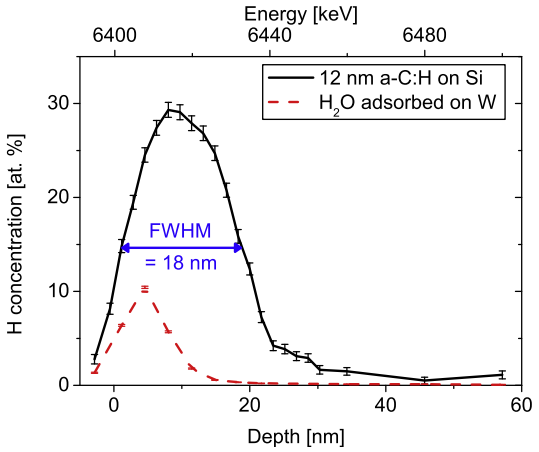

Fig. 5. Depth profiles of H in a 12 nm thick a–C:H film (solid curve) and a pure tungsten sample (dashed curve). FWHM is scetched into a–C:H depth profile (horizontal line).

578 keV. Taking this value and the known thickness of 330 nm, measured by ellipsometry, the stopping power of the a–C:H films can be determined to: $\frac{dE}{dx} = \frac{578\text{keV}}{330\text{nm}} = 1.75\,\frac{\text{keV}}{\text{nm}}$.

The hydrogen concentration is proportional to the count rate of gamma rays. Due to the sharp cross section, it is possible to calculate the hydrogen concentration with Eq. (6), where Y are the gamma ray counts, $\frac{dE}{dx}$ the stopping power and K a constant determined for the experimental setup [6]. The stopping powers used are the same as for the depth scale conversion.

$$c_{\text{hydrogen}} = K \cdot Y \cdot \frac{dE}{dx} \tag{6}$$

The hydrogen concentration of the analyzed samples are plotted in Fig. 5. On the tungsten sample an increase of the hydrogen concentration (calculated from the detected gamma rays) up to 10 at.% at an energy of 6408 keV is observed, followed by a drop to almost zero at 6432 keV. The NRA signals of the 12 nm a–C:H sample results in a hydrogen concentration around 25% from 6408 up to 6426 keV. At 6441 MeV it has droped to 4%.

On the bottom abscissa of Fig. 5 the energy scale has been converted to a depth scale. To determine the thickness of the thin a–C:H film, a Gauss function is fitted to the data. Its full-width-at-half-maximum ($FWHM_{\text{exp}}$) is 31.5 keV (18 nm), which is larger than the nominal thickness of 12 nm. This indicates an influence of the instrument function on this measurement. The width of this instrument function is determined by analysing the pure tungsten sample (dashed line in Fig. 5). Due to H_2O adsorbed on this sample, the H depth profile consists of a sharp peak at the surface. The width of this surface peak is not affected by stopping. A Gaussian fit to this peak yields a width of the instrument function ($FWHM_{\text{instrum}}$) of 15 keV, corresponding to a theoretical thickness of 4 nm in tungsten (stopping power: 3.86 keV/nm [9,11]) and 9 nm in a–C:H. Since both profiles can be reasonably described by Gaussians, the influence of the instrument function can be eliminated with formula (7).

$$FWHM = \sqrt{(FWHM_{\text{exp}})^2 - (FWHM_{\text{instrum}})^2} \tag{7}$$

The thickness of the thin a–C:H film is calculated by applying this equation and results in 27.7 keV (16 nm), which is in acceptable agreement with the known thickness of 12 nm.

5. Summary

The depth dependence of the experimentally achievable resolution of the ^{3}He NRA method is assessed. Well-defined test samples are used with D concentration profiles that can be described by delta functions at various depths. The experimental procedure and data evaluation are optimised using recently developed numerical programs based on Bayesian statistics. The resulting depth profiles broaden with increasing thickness of the coating. The apparent width of the D-containing layer represents the depth resolution for D that is achievable in this well-defined experiment with optimal conditions and with state-of-the-art data analysis. The results also show the dependence of the depth resolution on the atomic number of the cover layer, i.e. the matrix material. The trends and absolute values are compared to the theoretically achievable resolutions calculated with RESOLNRA.

For the characterization of the ^{15}N NRA method, a 12 nm a–C:H film, a 330 nm a–C:H film and a tungsten sample with adsorbed H_2O are analysed. The results show that the thickness of the 12 nm a–C:H-film is above the resolution limit of the ^{15}N method close to the surface. Compared to ^{3}He NRA this method has the clear advantage of a much reduced effort in data analysis, because no deconvolution of the experimental spectra is necessary. This enables a simple definition of the experimental depth resolution on the basis of the FWHM of the energy spread. The depth resolution of this method is being further explored in ongoing experiments on buried thin a–C:H films.

Acknowledgements

The authors at IPP Garching would like to thank Klaus Schmid, Matej Mayer and Udo von Toussaint for readily providing modified/extended versions of their numerical programs which were adapted to the specific requests of these investigations.

References

[1] M. Oberkofler, R. Piechoczek, Ch. Linsmeier, Phys. Scripta T145 (2011) 014011.
[2] V.Kh. Alimov, M. Mayer, J. Roth, Nucl. Instr. Meth. B 234 (2005) 169.
[3] M. Mayer, E. Gauthier, K. Sugiyama, U. von Toussaint, Nucl. Instr. Meth. B 267 (2009) 506.
[4] U. von Toussaint, T. Schwarz-Selinger, M. Mayer, S. Gori, Nucl. Instr. Meth. B 268 (2010) 2115.
[5] K. Schmid, U. von Toussaint, Nucl. Instr. Meth. B 281 (2012) 64.
[6] W.A. Lanford, Nucl. Instr. Meth. B 66 (1992) 65.
[7] T. Schwarz-Selinger, A. von Keudell, W. Jacob, J. Appl. Phys. 86 (1999) 3988.
[8] Roman Hartwich, Master's thesis, Hochschule München of Applied Sciences, 2008.
[9] A.F. Holleman, E. Wiberg, Lehrbuch der Anorganischen, Chemie (1995).
[10] F. Traeger, M. Kauer, Ch. Wöll, D. Rogalla, H.-W. Becker, Phys. Rev. B 84 (2011) 075462.
[11] M. Mayer, SIMNRA User's Guide, Report IPP 9/113, Max-Planck-Institut für Plasmaphysik, Garching, Germany, 1997. Available from: <http://www.rzg.mpg.de/mam/>, mailto:matej.mayer@ipp.mpg.de
[12] M. Mayer, Nucl. Instr. Meth. B 266 (2008) 1852.